European Journal of Pharmaceutical Sciences 178 (2022) 106280

Contents lists available at ScienceDirect

European Journal of Pharmaceutical Sciences

journal homepage: www.elsevier.com/locate/ejps

Structured approach for designing drug-loaded solid products by binder jetting 3D printing

Yingya Wang [a,b], Anette Müllertz [a], Jukka Rantanen [a,*]

[a] Department of Pharmacy, Faculty of Health and Medical Sciences, University of Copenhagen, Copenhagen, Denmark
[b] Mille International ApS, Hellerup, Denmark

ARTICLE INFO

Keywords:
Pharmaceutical products
Oral drug delivery
Binder jetting 3D printing
Quality by Design

ABSTRACT

Additive manufacturing allows for designing innovative properties to pharmaceutical products. Binder jetting (BJ) 3D printing is one of the key techniques within innovative manufacturing. In this study, a structured approach according to the Quality by Design (QbD) principles was implemented to explore the factors affecting fabrication of drug-loaded products produced by BJ 3D printing. The investigated factors included the weight ratio of binder in primary powder and the process parameters related to printing (layer thickness and number of layers). Critical quality attributes, namely disintegration time, tensile strength, friability, dimensions (diameter and height accuracies), residual water content, weight and drug loading were determined based on the quality target product profile of a tablet analogue. The experimental results with a 2-level full factorial design were modeled by multiple linear regression. It was found that binder content was an important factor determining the integrity of the printed products, and the formation of the microstructure of the product was affected by multiple material properties and process parameters. QbD is a systematic and effective approach providing mechanistic understanding of BJ 3D printing and allowing for an efficient design of products with the desired quality.

1. Introduction

Additive manufacturing (AM) is getting an increasing attention as an approach to develop and fabricate pharmaceutical products. AM refers to a construction of an object in a successive layer-upon-layer manner. It has several advantages compared with traditional manufacturing, such as the flexibility to rapid prototyping and small-scale manufacturing. Additional benefit is the ability to fabricate products with complex geometry and tailored microstructure. During the past decades, pharmaceutical products based on AM have demonstrated its possibility to fabricate drug delivery systems that cannot be achieved by conventional pharmaceutical manufacturing processes (Trenfield et al., 2018, Lepowsky and Tasoglu, 2018, Goole and Amighi, 2016, Prasad and Smyth, 2016). Binder jetting (BJ) 3D printing is a powder-based AM method. The primary powder, which refers to feeding powder mixture loaded in the BJ printer forming the powder bed, typically contains active pharmaceutical ingredient(s) (APIs) and various functional excipients such as inactive matrix material(s). The liquid binder, which is also called ink, is sprayed onto the powder bed in a designed pattern with a goal to bind powder material into a solid object. Another strategy is to add a solid binder in the primary powder, which will subsequently get partially dissolved by the sprayed ink used for binding. Several drug delivery systems have been successfully fabricated by BJ, with examples covering personalized medicine, multicompartmental/multi release drug delivery devices, high/low drug loaded pharmaceutical products, and orodispersible formulations (Sen et al., 2021, Rahman et al., 2020).

Structured and risk-based drug development work is a key to successful design of pharmaceutical products. Quality by Design (QbD) is a well-established approach that emphasizes the focus on quality of the product early in drug development process (Yu et al., 2014, Juran, 1992). It is especially important to implement QbD to the development of novel products, such as the AM-based innovative drug delivery

Abbreviations: ACN, Acetonitrile; AM, Additive manufacturing; APIs, Active pharmaceutical ingredients; BJ, Binder jetting; CMAs, Critical material attributes; CPPs, Critical process parameters; CQAs, Critical quality attributes; DoE, Design of Experiments; HPLC, High-performance liquid chromatography; IBU, Ibuprofen; MLR, Multiple linear regression; Num, Layer number; PCM, Paracetamol; Ph. Eur., European Pharmacopoeia; PVP, Polyvinylpyrrolidone; QbD, Quality by Design; QTPP, Quality target product profile; SEM, Scanning electron microscopy; TGA, Thermogravimetric analysis; Thk, Layer thickness.

* Corresponding author at: Department of Pharmacy, Faculty of Health and Medical Sciences, University of Copenhagen, Universitetsparken 2, 2100 Copenhagen, Denmark.

E-mail address: jukka.rantanen@sund.ku.dk (J. Rantanen).

https://doi.org/10.1016/j.ejps.2022.106280
Received 12 April 2022; Received in revised form 11 August 2022; Accepted 16 August 2022
Available online 28 August 2022

systems. QbD is underlining the importance of product and process understanding. Key elements in this are to identify the statistically significant correlations and explain the observed phenomena at a mechanistic level, instead of merely listing the statistical parameters. It is a common misconception of QbD to consider this approach only as a statistical exercise without including the mechanistic explanation. BJ 3D printing is still a relatively new technique in the pharmaceutical context, and there is only limited number of published work focusing on key principles determining the formation of a drug-loaded solid product within this processing solution.

In this work, a structured approach according to the QbD principles was used to explore the BJ 3D printing. The targeted product was an analogue of a pharmaceutical tablet for oral delivery. The quality target product profile (QTPP) of the product was defined, followed by a qualitative risk assessment on BJ 3D printing process. Material selection and process parameters were investigated with Design of Experiments (DoE) to identify their criticality to examined critical quality attributes. A special focus was on linking the experimental findings to a mechanistic understanding of the general factors determining the quality of BJ 3D printed products.

2. Materials and Methods

2.1. Materials

The model drugs, ibuprofen (IBU) and paracetamol (PCM), were obtained from Fagron A/S (Copenhagen, Denmark). Polyvinylpyrrolidone (PVP), Kollidon® 30 was purchased from BASF Corporation (Ludwigshafen, Germany). SuperTab® 11SD lactose monohydrate (lactose) was donated by DFE Pharma (Goch, Germany). The high-performance liquid chromatography (HPLC) grade ethanol and acetonitrile (ACN) were from VWR Chemicals (Radnor, PA, US). Water used in this study was purified by Ultra Clear™ reverse osmosis system from Evoqua Water Technologies (Barsbüttel, Germany).

The primary powder comprised one model drug, PVP, and lactose. All the compositions of primary powder were mixed in Turbula® shaker-mixer (Willy A. Bachofen AG, Muttenz, Switzerland) at 35 rpm for 5 minutes. Ink solution used for printing was either water based or water-ethanol co-solvent based systems. All the ink solution contained 5% w/V of PVP to reach the viscosity for a stable spray (Fromm, 1984).

In the *Screening study* of this work, the composition of primary powder is indicated in the sample code in the following way API_DrugLoad:PVP:Lactose_EthInk. For example, a code of PCM_3:1:6_0 refers to the primary powder comprised 30% w/w of PCM, 10% w/w of PVP, and 60% w/w of lactose, and the ink was based on water without ethanol. In the *Optimization study*, the layer thickness (Thk)*layer number (Num) is indicated, such as API_DrugLoad:PVP:Lactose_Thk*Num.

2.2. Design of Experiments

The factors including critical material attributes (CMAs) and critical process parameters (CPPs) for a printable product by BJ were analyzed in the risk assessment and visualized with an Ishikawa diagram. Selected factors were explored in the following DoE for their impacts on the critical quality attributes (CQAs) related to a QTPP of the current product of an oral tablet. The *Screening study* and the *Optimization study* were designed with MODDE 12.1 (Umetrics AB, Umeå, Sweden), with a goal to identify the link between CQAs and selected CMAs and CPPs.

The *Screening study* on two APIs, i.e., IBU and PCM, was designed by using the full factorial (2 levels) interaction model with triplicate at the center point, investigating three factors, namely, the drug content in primary powder, the binder content in primary powder, and the ethanol content in ink (Table 1). Hence, there were 22 runs in the *Screening study*, and all were executed in a random order generated by the software MODDE.

Table 1
Levels of composition factors in the Screening study of ibuprofen and paracetamol.

Factor	Type	Low (-1)	Centre (0)	High (+1)
Drug loading (w/w)	Quantitative	10%	20%	30%
Binder content (w/w)	Quantitative	10%	20%	30%
Ethanol in ink (V/V)	Quantitative	0	10%	20%

The *Optimization study* was subsequently designed according to results from the *Screening study*, where primary powder composition with high drug loading (*Screening study*, 30% w/w of PCM) and aqueous ink without ethanol were further studied. Three factors, namely, the binder content in primary powder and two process factors (layer thickness and layer number) were investigated by the same interaction model (Table 2). There were 11 runs in the *Optimization study*, and all were executed in a random order generated by MODDE.

2.3. Particle size

Particle size and size distribution of raw materials were measured with Malvern Mastersizer 2000 using a Scirocco dry sampling system (Malvern Panalytical Ltd., Malvern, UK). The vibration of feeding plate was 50% intensity, and the dispersive air pressure was at 3 bar. The obscuration was within 0.5 to 6%. Particle size at 10%, 50% and 90% fractiles was presented as D10/D50/D90 (μm). Span was calculated by Eq (1).

$$\text{Span} = \frac{\text{D90} - \text{D10}}{\text{D50}} \quad (1)$$

2.4. Binder jetting 3D printing

According to the DoE plan, different compositions of primary powder and ink solution were printed into designed shapes (simple cylinder of different heights, designed by TinkerCAD, Autodesk, Inc., San Rafael, CA, US) by Easy3DP-M300 printer (EasyMade, Wuhan, China). The controlling and pattern slicing software installed in the system is Easy3DColor by EasyMade. For the 22 runs in the *Screening study*, the printed products were designed as a cylinder of 12 mm in diameter and 2 mm in height with the layer thickness of 0.10 mm. For the 11 runs in the *Optimization study*, the diameter of products was still 12 mm, but the height varied as layer thickness and number of layers were two investigated factors. Other process parameters and the environmental condition were at a constant level for all the printing experiments, including the roller spreading speed of 10 m/minute and rotation rate of 10 pulse/second, as well as room temperature at 25 °C and room humidity at 55 ± 3% of relative humidity. The ink was sprayed from 4 rows of 320 nozzles in Gen5 MH5420 piezoelectric printhead (Ricoh China Ltd., Shanghai, China) at a fixed volume of 3.2 to 3.4 μl per product per layer. The vacuum pressure of ink cartridge was ranging from -0.4 to -0.6 kPa. In both the *Screening study* and the *Optimization study*, successfully solidified products were dried for 12 hours at 50 °C and collected afterwards by removing the powder residue manually.

Table 2
Levels of composition and process factors in the Optimization study of paracetamol.

Factor	Abbreviation	Type	Low (-1)	Centre (0)	High (+1)
Binder content (w/w)	PVP	Quantitative	10%	20%	30%
Layer thickness (mm)	Thk	Quantitative	0.10	0.15	0.20
Layer number	Num	Quantitative	30	35	40

2.5. Thermogravimetric analysis

The residual water content of the printed products from the *Optimization study* was measured by thermogravimetric analysis (TGA) after they were dried and collected. Around 5 mg of sample was placed in a tared platinum pan and subsequently heated from 30 to 120 °C at a rate of 10 °C/minute with nitrogen purging in TGA 5500 from TA Instruments (New Castle, DE, US). The percentage of weight loss during the heating was recorded. The test was performed in triplicate for each composition. As a reference, raw powder of PCM, PVP, and lactose was measured by the same method.

2.6. Scanning electron microscopy

The printed products from the *Optimization study* were manually dissected vertically to the circular plane with a scalpel. Samples were coated with gold for 20 seconds by Cressington 108 Auto sputter coater from Ted Pella, Inc. (Redding, CA, US) under argon purging. The exposed face by dissection was observed by TM3030 scanning electron microscopy (SEM) from Hitachi (Tokyo, Japan). Images were taken with an accelerating voltage of 5 kV.

2.7. Disintegration

The disintegration time of printed products from the *Optimization study* was measured in PTZ 2E disintegration apparatus (Pharma Test, Hainburg, Germany) according to the basket-rack method from European Pharmacopoeia (Ph. Eur.) 2.9.1 (European Pharmacopoeia Commission, 2019).

2.8. Weight, size, and tensile strength

Six products from each successfully printed composition in both the *Screening study* and the *Optimization study* were weighted and dimensional measured in diameter and height by using a vernier caliper. The diameter and height accuracies were indicated by the ratio of measured size to the designed size expressed as percentages. Subsequently products were placed in Dr. Schleuniger Pharmatron tablet tester 8M (SOTAX AG, Aesch, Switzerland) for measuring the diametral crushing strength. In the *Optimization study*, tensile strength was used for further analysis, which was calculated based on sample diametral crushing strength, diameter, and height by Eq (2).

$$\text{Tensile strength} = \frac{2 \times \text{Diametral crushing strength}}{\pi \times \text{Diameter} \times \text{Height}} \quad (2)$$

2.9. Friability

Friability of successfully printed products from the *Optimization study* was tested by a modified Ph. Eur. 2.9.7 method (European Pharmacopoeia Commission, 2019) using a standard drum apparatus equipped with motor (Parvalex, Greve, Denmark). Since products from different compositions varied in weight, a sample of whole products corresponding to a modified weight range from 6.2 to 6.8 g, instead of 6.5 g, was collected and weighed. Products were placed in the drum for 100 times rotation in 4 minutes. After test, products were carefully dedusted and weighed again to calculate the percentage of weight loss. The test was performed in triplicate for each composition.

2.10. Dissolution and drug loading

The dissolution of printed products from the *Optimization study* was measured in a paddle apparatus (DT 700, ERWEKA GmbH, Langen, Germany) based on the method from Ph. Eur. 2.9.3 (European Pharmacopoeia Commission, 2019). The weight of each printed product was firstly determined. Samples were placed at the bottom of vessel containing 500 ml water at 37 ± 0.5°C with a paddle rotating at a speed of 50 rpm. 2 ml supernatant was taken at predetermined time points (1, 5, 10, 30, and 60 minute) and stored for quantitative analysis. After sampling, fresh water of the same volume was added. Medium of all the samples at time point of 24 hour was collected for calculating drug loading, assuming all the loaded drug has been dissolved and released. The test was performed in triplicate for each composition.

2.11. Quantitative analysis

The selected API in the *Optimization study*, PCM, was quantified by a HPLC method using Agilent 1260 Infinity instrument (Agilent Technologies, Santa Clara, CA, US) installed with a reverse phase C18 column (Kinetex® 00D-4462-AN, Phenomenex, Inc., Torrance, CA, US). Dissolved samples were pretreated by filtering through a 0.45 μm nylon syringe filter (Frisenette Aps, Knebel, Denmark). The mobile phase was mixture of water-ACN (90:10, V/V) pumped at a constant flow rate of 0.15 ml/minute at 25 °C. To each HPLC run, 5 μl sample was injected. At the retention time of 4.2 minute, peak detected at 254 nm by 1290 Diode Array detector (Agilent Technologies, Santa Clara, CA, US) was identical to PCM, and its area under curve was recorded. The R^2 of calibration (n=3) on PCM at concentration from 0.005 to 0.360 mg/ml was 0.9991, and all the concentrations of determined samples were within this range.

2.12. Statistics

All the statistical analysis of the DoE results was performed in MODDE. Multiple linear regression (MLR) was used to fit data. Non-significant model terms were removed. Significance test was conduct by Student's t-test with a confidence interval of 95%.

3. Results and discussion

3.1. Risk overview

The printed products were designed to be an analogue of oral tablet that meets basic requirements defined by Ph. Eur. The QTPP of a printed product together with the CQAs is summarized and justified in Table 3. In this work, the focus was on the CQAs related to disintegration, mechanical hardness, friability, uniformity of dimensions, residual solvent,

Table 3
An overview of the quality target product profile (QTPP) and critical quality attributes (CQAs) of the printed product as an analogue of oral tablet.

Quality attribute	Target	Justification
Dosage form	Solid product for oral administration	The printing process should be robust and controllable.
Appearance	An analogue of uncoated tablet	The targeted product is in shape of a solid cylinder, same as a normal pharmaceutical tablet.
Disintegration	≤ 15 minutes	As for an uncoated immediate release tablet, according to Ph. Eur. 2.9.1[a]
Tensile strength	At a relevant level based on product	This should be in a range that the product is hard enough to resist crushing during handling, packaging, transporting, and distributing, but not too strong to disintegrate.
Friability	≤ 1%	Ph. Eur. 2.9.7[a]
Residual solvent	Complying with ICH guideline Q3C R8 (Q3C (R8) Residual solvents)	-
Weight	≤ 5% weight deviation (for product ≥ 250 mg per unit)	Ph. Eur. 2.9.5[a]
Drug loading	≤ 15% drug loading deviation	Ph. Eur. 2.9.6[a]

[a] Ph. Eur.: European Pharmacopoeia, 10th Edition, 2019.

and drug loading. To obtain a solid product with targeted quality attributes, it is necessary to investigate the relevant factors in BJ process that determine the QTPP, and further, to identify the underlying mechanisms related to each CQA.

Factors affecting the properties of a printable product by BJ are visualized and presented in an Ishikawa diagram (Fig. 1). A general BJ 3D printing process is powder-based (Mostafaei et al., 2021), hence the quality of a printable product is affected by the solid material composing the primary powder and the liquid material of ink. A key material affecting the powder binding is binder, which can be either a part of the solid material or dissolved in the liquid phase (Chang et al., 2020), and the binder selection is specifically mentioned in the Ishikawa diagram. The technical parameters and specifications of mechanical parts including the printer and the installed printhead are also important to process. Some printer-related parameters can be controlled in the printer by user to optimize the printing process. These usually include the printing pattern and array, layer thickness and number, roller spreading and rotation speed, as well as the printhead moving speed and direction (Lu and Reynolds, 2008). The environment influence during fabrication and the post-process procedure are another two factors determining the success of printing.

Based on this cause-and-effect diagram, a simple product was designed comprising a model drug, a binder of PVP, and a matrix of lactose. As mentioned earlier, two powder systems with either IBU or PCM were prepared. PVP was selected because it is a widely used hydrophilic binder in BJ 3D printing of pharmaceutical products (Chang et al., 2020, Sen et al., 2020, Wilts et al., 2019, Tian et al., 2019, Tian et al., 2018, Yu et al., 2009, Wang et al., 2006, Lee et al., 2003, Rowe et al., 2000). Modified spherical lactose was selected in this research work due to its reported good performance in BJ (Chang et al., 2020, Sen et al., 2020, Wilts et al., 2019, Tian et al., 2019, Yu et al., 2009, Rowe et al., 2000). It can assist the process of powder spreading and act as the filler in pharmaceutical products to achieve the targeted drug loading. In the *Screening study*, besides the type of API, weight ratio of solid materials and the type of ink were explored as factors, and in the *Optimization study*, the weight ratio of binder and product dimensions were studied, which are factors indicated in red font in Fig. 1. Other factors, namely, the printer and printhead, parameters for the printing process, environment, and post-process also determined the printability of BJ process in this study, which were set within an optimal range according to preliminary studies, hence they were not further explored.

3.2. Screening study

The *Screening study* was a starting point to evaluate the printing feasibility of the two model drugs together with PVP and lactose in the primary powder. IBU and PCM are two painkiller drugs with different physical properties, such as melting point (IBU 78°C, PCM 169°C), aqueous solubility (IBU 0.021 mg/ml, PCM 14 mg/ml, room temperature), and particulate properties, e.g., particle size and size distribution (Table S1). At this stage, the evaluation focused on the printing feasibility. Only two samples (PCM_3:1:6_0 and PCM_3:3:4_0) could be successfully printed and collected (Table S2). Three types of failure modes of printing were observed, namely, size expansion, groove, and fragile (Table S2), which are discussed below.

3.2.1. Ibuprofen products

None of the IBU samples was printable, because size expansion and groove with powder spreading occurred in the printed powder area. Size expansion was observed as the detaching of the wetted area from powder bed (Fig. 2A). When the volume of sprayed ink is not optimal considering the porosity and the solubility of primary powder, saturation occurs at the surface leading to an increase in the surface roughness degree (Mostafaei et al., 2021, Lu and Reynolds, 2008). Consequently, the friction force from fresh powder during spreading increases, and the printed area is pushed forward with the fresh powder spreading, which causes groove along with powder spreading direction (Fig. 2B). Additionally, if the printing process is too fast to let the surface of wetted powder get dried, there is a tendency for the wetted powder to bind the fresh powder during powder spreading. This often happens in the beginning of the process (at the firstly printed several layers), because mass of the printed lamination is not large enough to resist the friction generated by powder spreading. Different from the case of size expansion where the printing can still proceed, the groove destroys previously printed area and impedes the printing process immediately. In SEM images of the two examples, IBU_3:3:4_0 (Fig. 2C) had less pores than IBU_3:1:6_0 (Fig. 2D). This is consistent with the fact that PVP acts as the binder in primary powder and contributes to the formation of solid bridges. It can also be observed from SEM images that the appearance of IBU crystals was not changed by the process, which indicates IBU particles barely participated in the formation of solid bridges during solidification. It can be concluded that printing of low soluble drug compound can be challenging, and particle engineering is necessary (Kozakiewicz et al., 2021).

3.2.2. Paracetamol products

With the same printing conditions, two PCM samples PCM_3:1:6_0 and PCM_3:3:4_0 were printable (Fig. 3A). When using 20% V/V ethanol co-solvent system, printing could be performed, but the obtained products were too fragile for further analysis (Fig. 3B). Although PVP is freely soluble in both water and ethanol, ethanol can reduce the solubility of lactose (Majd and Nickerson, 1976), which limits the formation of solid bridges during solidification. The SEM images show PCM_3:3:4_20% (Fig. 3F) was more porous with more undissolved particles than PCM_3:3:4_0 (Fig. 3E).

In the experiments with 10% and 20% w/w of PCM in the primary powder (Fig. 3C and Fig. 3D), both size expansion and groove were observed, while 30% w/w of PCM products did not have this problem,

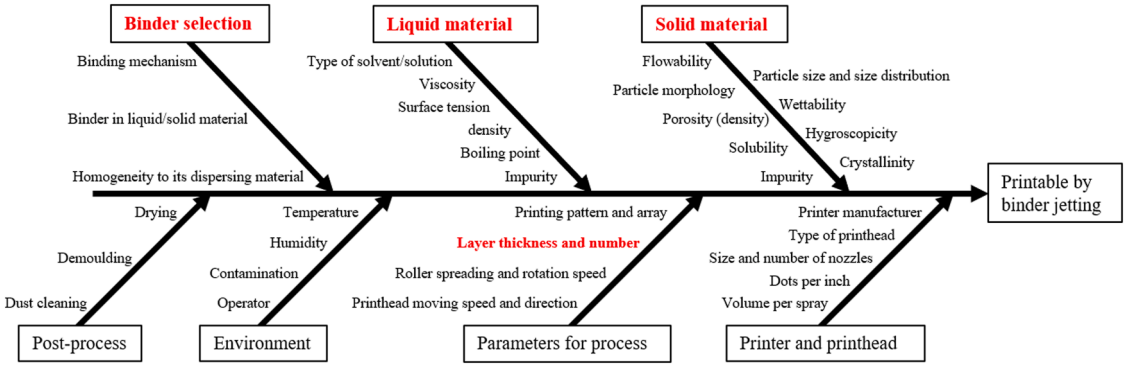

Fig. 1. Ishikawa diagram of factors in binder jetting 3D printing to the outcome of a printable product. The factors marked in red were explored in this study. (For interpretation of the references to colour in this figure legend, the reader is referred to the web version of this article.).

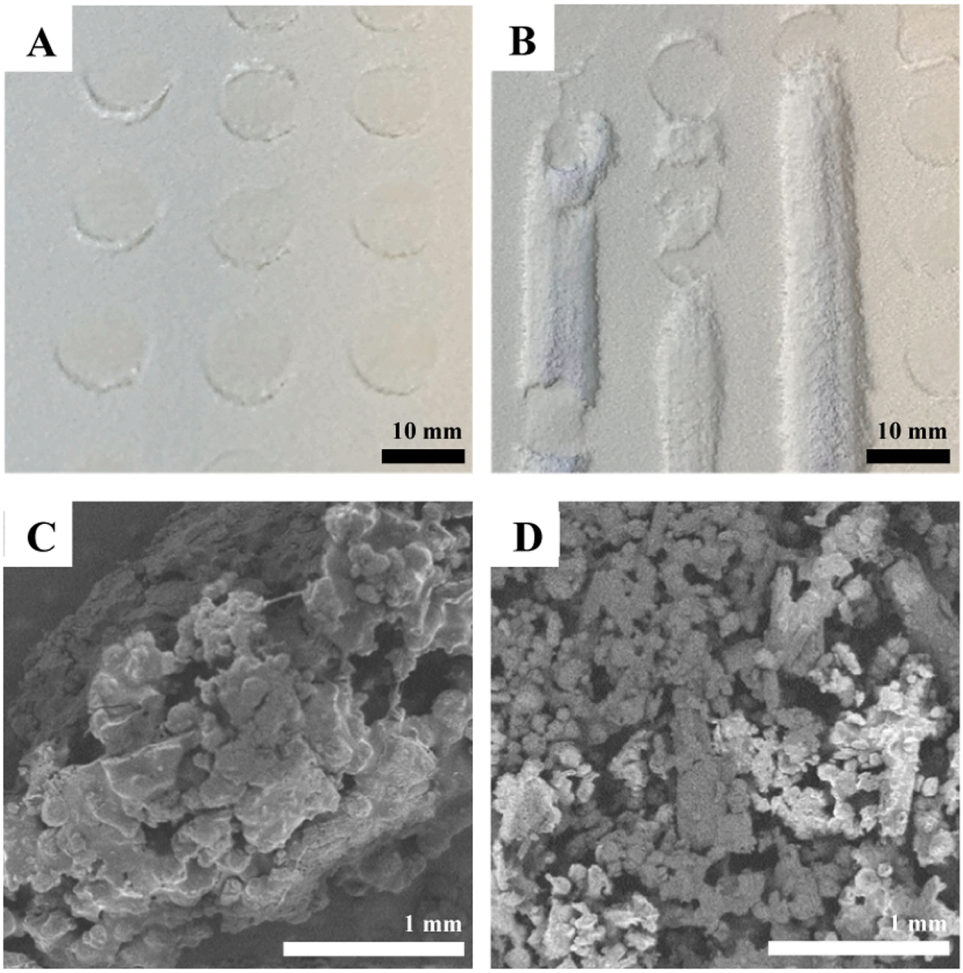

Fig. 2. Examples of failure modes in printing of ibuprofen (IBU) products (A) IBU_3:3:4_0 and (B) IBU_3:1:6_0. The failure was caused by size expansion and groove on printing area. (C) IBU_3:3:4_0 and (D) IBU_3:1:6_0 are SEM images of the two samples. Sample code follows Drug_DrugLoad:Polyvinylpyrrolidone:Lactose_Ethanol % in Ink.

which indicates the weight ratio of PCM in primary powder was a critical factor for printing. PVP and lactose used in this work are commercially modified products for general tableting purpose, and they are of similar particle size with a narrow size distribution (span < 2, Table S1). The measured D50 of PVP and lactose was around 50 μm, which is in the optimal range of 30-50 μm for BJ processing reported by Antic *et al.* (Antic et al., 2021, Antic et al., 2018), and D90 of PVP and lactose was slightly higher than the layer thickness of 0.10 mm. However, this is consistent with the observation from Infanger *et al.* (Infanger et al., 2019) who stated particles that were 17 μm larger than the layer thickness could still be printed. The model drug PCM had a relatively broad size distribution (span > 7, Table S1). D10, D50, and D90 of PCM were all smaller than those of PVP and lactose. Several studies have identified that using primary powder with a bimodal size distribution is an effective way to increase the powder bed density (Mostafaei et al., 2021, Miyanaji et al., 2018, Bai et al., 2015, Zhou et al., 2014). Fine particles in primary powder fill voids between big coarse particles and provide more binding sites (German and Park, 2008), and consequently they improve physical integrity and strength of printed products (Mostafaei et al., 2021, Miyanaji et al., 2018, Bai et al., 2015, Tan et al., 2017, Bai et al., 2017, Spath et al., 2015, Lanzetta and Sachs, 2003). The primary powder containing 30% w/w of PCM had two apparent peaks in particle size distribution (Fig. S1), which might explain why only 30% w/w of PCM samples were printable in this work. On the other hand, powder with bimodal size distribution may result in segregation (Infanger et al., 2019). This could cause the loss in drug loading of printed products, which is discussed in *3.3.2 Critical factors affecting the properties of printed product*.

In the representative SEM images, 10% and 20% w/w of PCM samples (Fig. 3G and Fig. 3H) contained more unbound lactose particles and void space than 30% w/w of PCM sample (Fig. 3E). In the 30% w/w of PCM sample, crystals of PCM were visible and distributed among dissolved PVP clots being a part of solid bridges. This visually supports the finding that the density of BJ product is improved by using powder with a bimodal size distribution. Nearly unimodal size distribution might be one more cause for failures in printing IBU products besides the influence from solubility, as particle size of IBU, comparing with PCM, is closer to particle size of PVP and lactose (Table S1).

The successfully printed products of PCM_3:1:6_0 and PCM_3:3:4_0 were collected and tested on crushing strength. There was no significant difference (P-value=0.0669) between the two samples, but they were generally too soft for further analysis.

3.3. Optimization study

3.3.1. Characteristics of optimized products

In the *Optimization study*, 30% w/w of PCM in primary powder and the ink system with 5% w/V PVP aqueous solution were used. To increase the hardness of printed products, the number of layers was increased and investigated between 30 and 40 layers, and the layer thickness was explored between 0.10 and 0.20 mm. In the *Optimization study*, all the 11 primary powders were successfully printed (Fig. 4) and

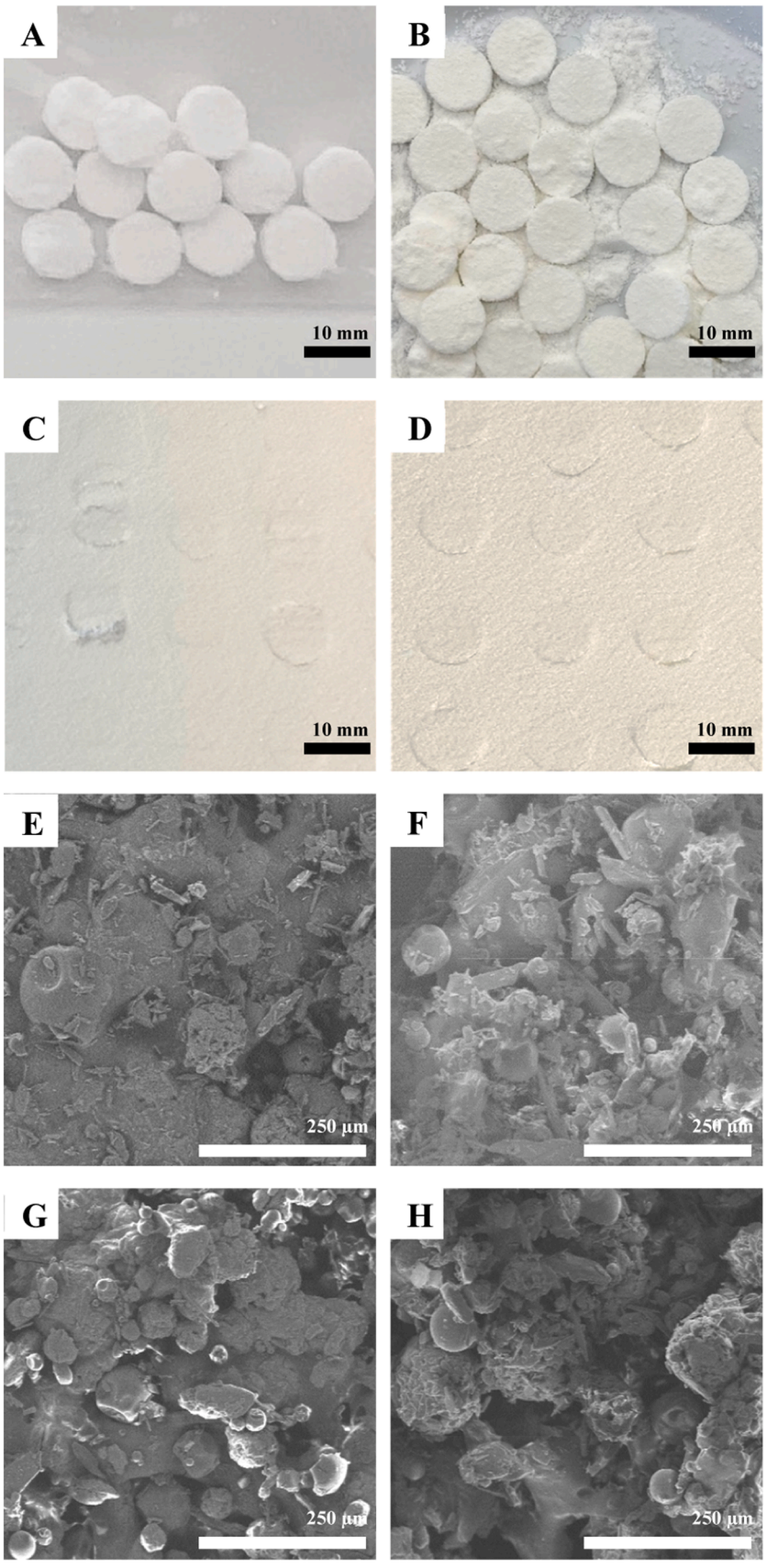

Fig. 3. Examples of paracetamol (PCM) products. (A) successfully printed example of PCM_3:3:4_0, (B) fragile example of PCM_3:3:4_20%, (C) groove example of PCM_1:3:6_0, and (D) size expansion example of PCM_2:2:6_10%. SEM images of (E) PCM_3:3:4_0, (F) PCM_3:3:4_20%, (G) PCM_1:3:6_0, and (H) PCM_2:2:6_10% are shown correspondingly. Sample code follows Drug_DrugLoad:Polyvinylpyrrolidone:Lactose_Ethanol% in Ink.

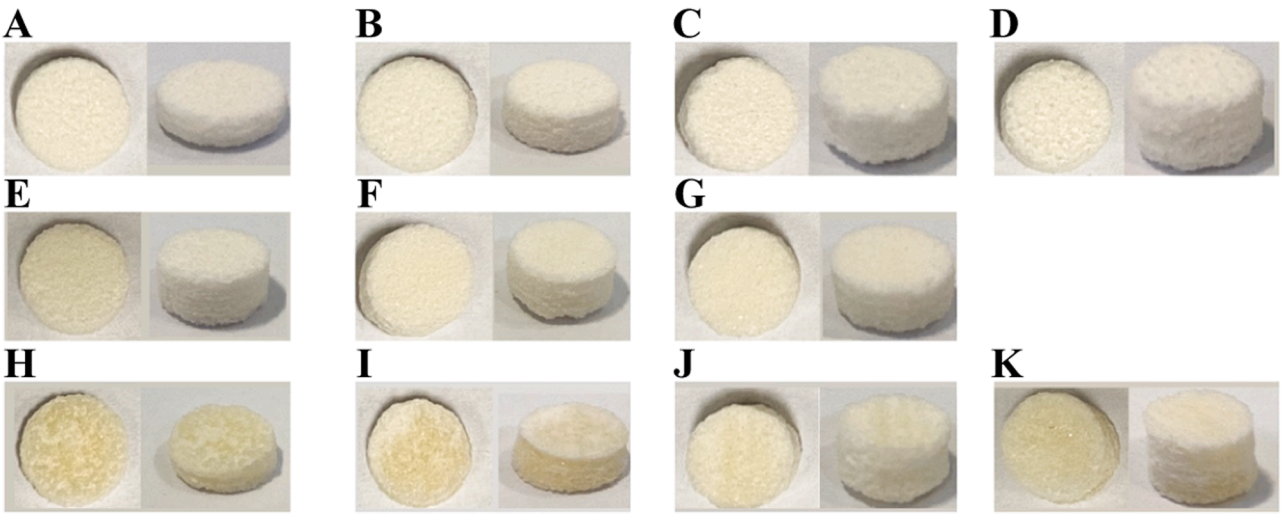

Fig. 4. Printed paracetamol (PCM) products in the *Optimization study*, in the order of (A) PCM_3:1:6_0.10 mm*30, (B) PCM_3:1:6_0.10 mm*40, (C) PCM_3:1:6_0.20 mm*30, (D) PCM_3:1:6_0.20 mm*40, (E), (F) and (G) PCM_3:2:5_0.15 mm*35, (H) PCM_3:3:4_0.10 mm*30, (I) PCM_3:3:4_0.10 mm*40, (J) PCM_3:3:4_0.20 mm*30, (K) PCM_3:3:4_0.20 mm*40. The diameter of all products is approximately 12 mm. Sample code follows Drug_DrugLoad:Polyvinylpyrrolidone:Lactose_LayerThickness*LayerNumber.

characterized (Table 4).

General appearance of all the 11 compositions of printed products was similar to the designed tablet shape, although size shrinkage and expansion could be observed. All the products were strong enough for collecting and further analysis. The disintegration time of 10% and 20% w/w of PVP samples was within 3 minutes, which would be ideal for an orodispersible product. Especially, the 10% w/w of PVP samples showed a fast disintegration within 10 seconds. For the 30% w/w of PVP samples, the disintegration time was within 30 minutes. However, the friability of all the printed samples was more than the 1% weight loss as required by Ph. Eur. The poor friability is a common problem in BJ 3D printing pharmaceutical products (Tian et al., 2019, Lee et al., 2003, Antic et al., 2021, Yu et al., 2009). Comparing with conventional compacted tablets, BJ-based processing does not allow for formation of interparticulate interactions via brittle and plastic deformation (Vromans et al., 1985), which contributes to a porous microstructure in products but compromises the product induration. The problem with friability can also be related to the large particle size of the primary powder (Infanger et al., 2019). The issue on product quality caused by the poor friability can be mitigated with in-cavity printing technology by which each BJ product is fabricated directly in an individual blister that is immediately packaged after printing (Beach-Herrera et al., 2019). There is an obvious need for novel formulation strategies to solve this challenge without all too complicated packaging solutions.

Dissolution behavior of all the samples was further studied. Since the disintegration time of 10% w/w of PVP samples was remarkably shorter than that of 20% and 30% w/w of PVP samples, the dissolution profiles were presented by the binder content (Fig. S2). All the samples released more than 90% of drug within 1 hour. PCM was released relatively slower from the 30% w/w of PVP samples than others, which is related to not only the slow disintegration but also the retarding effect from PVP. PVP is a well-known viscosity-increasing agent, and during

Table 4
Characterization results of printed paracetamol (PCM) products from the Optimization study. Sample code follows Drug DrugLoad:Polyvinylpyrrolidone:Lactose_-LayerThickness*LayerNumber. Values are presented by mean ± standard deviation, n=3 or 6 according to each method.

Sample code	Disintegration time (s)	Crushing strength (N)	Tensile strength (MPa)	Friability (weight loss, %)	Diameter accuracy (%)	Height accuracy (%)	Residual water content (%)	Weight (mg)	Drug loading (%)
PCM_3:1:6_0.10 mm*30	6 ± 1	51 ± 13	0.7 ± 0.2	8.6 ± 1.5	102.0 ± 1.2	136.6 ± 4.0	1.0 ± 0.0	297.1 ± 15.0	104.5 ± 0.7
PCM_3:1:6_0.10 mm*40	7 ± 1	34 ± 5	0.3 ± 0.0	13.3 ± 0.9	101.4 ± 1.6	126.8 ± 5.6	1.0 ± 0.0	331.1 ± 8.8	104.2 ± 1.6
PCM_3:1:6_0.20 mm*30	6 ± 1	36 ± 12	0.3 ± 0.1	17.4 ± 1.2	100.8 ± 1.7	114.9 ± 2.4	0.9 ± 0.1	388.3 ± 23.2	98.7 ± 1.8
PCM_3:1:6_0.20 mm*40	7 ± 1	26 ± 7	0.2 ± 0.0	21.5 ± 1.9	100.9 ± 0.9	105.2 ± 2.9	0.9 ± 0.1	433.7 ± 37.2	97.8 ± 1.3
PCM_3:2:5_0.15 mm*35	116 ± 17	67 ± 12	0.6 ± 0.1	6.1 ± 1.2	99.2 ± 1.1	120.8 ± 3.5	1.6 ± 0.1	423.9 ± 8.3	96.1 ± 3.7
PCM_3:2:5_0.15 mm*35	103 ± 13	92 ± 16	0.8 ± 0.1	5.2 ± 0.9	96.6 ± 1.9	119.0 ± 4.5	1.5 ± 0.1	431.6 ± 14.0	99.4 ± 2.6
PCM_3:2:5_0.15 mm*35	130 ± 31	140 ± 13	1.1 ± 0.1	3.6 ± 1.0	98.8 ± 1.0	128.0 ± 6.5	1.3 ± 0.1	475.9 ± 28.9	99.3 ± 3.1
PCM_3:3:4_0.10 mm*30	761 ± 32	145 ± 21	2.1 ± 0.4	7.7 ± 0.5	98.5 ±1.4	124.2 ± 10.1	0.9 ± 0.0	320.6 ± 27.3	100.6 ± 2.0
PCM_3:3:4_0.10 mm*40	1036 ± 95	174 ± 28	1.9 ± 0.3	4.3 ± 0.4	98.3 ± 2.4	123.8 ± 10.3	1.4 ± 0.1	452.4 ± 24.1	96.0 ± 1.2
PCM_3:3:4_0.20 mm*30	1190 ± 244	210 ± 39	1.8 ± 0.3	3.3 ± 0.5	92.6 ± 2.2	108.8 ± 9.0	1.2 ± 0.3	511.2 ± 64.0	97.2 ± 1.8
PCM_3:3:4_0.20 mm*40	1447 ± 481	262 ± 28	1.9 ± 0.2	5.1 ± 0.8	88.1 ± 2.9	102.5 ± 1.9	1.6 ± 0.2	586.4 ± 22.5	89.9 ± 1.2

dissolution it can form viscous barrier surrounding the sample in media that slows down the overall dissolution. It should be highlighted that since BJ requires much higher content of PVP in the product than the conventional compacted products that typically contain 0.5-5% w/w of PVP (Guy et al., 2009). The impact on dissolution related to the high amount of PVP in products should be taken into consideration when designing a BJ pharmaceutical product. This is underpinning the importance for identifying strategies for reducing the amount of binder (PVP) in the pharmaceutical product.

3.3.2. *Critical factors affecting the properties of printed product*

Results from Table 4 were analyzed with the MLR model, and the procedure is described in the Supplementary information. The coefficients of significant factors related to the responses for all the successful models are presented in Table S3.

It was observed that within the investigated design space, the disintegration time and tensile strength of products were logically positively correlated to the binder content, and the weight loss during friability test was negatively correlated to the binder content. This proved the binder (PVP) plays an essential role in product solidification and integrity, and the poor friability of samples can be improved by increasing the content of PVP in primary powder. The responses of tensile strength and friability were strongly related (|correlation value|>0.8) to the response of disintegration time as indicated in Table S4.

The diameter accuracy was affected by the binder content, layer thickness, and the interaction of these two factors, while the height accuracy was only affected by the layer thickness. Based on the numeric results in Table 4, both shrinkage and expansion in size were observed on printed products at horizontal direction, but only expansion happened at vertical direction. In the model of diameter accuracy, the results indicate that samples with 10% w/w of PVP expanded slightly at the horizontal direction, and with the increase on layer thickness, this expansion was less dominant. However, for the samples with more PVP in the primary powder, shrinkage at the horizontal direction occurred. Shrinkage in size is an expected phenomenon in BJ, because the binder forms solid bridges linking particles after drying, which reduces the void space between particles leading to a decrease in porosity (Mostafaei et al., 2021). This is consistent with the observation in this study, i.e., a high binder content in primary powder leading to a large extent of shrinkage. Simultaneously, the size expansion can occur when too high volume of ink is used. In the model of height accuracy, the thinner layer was, the greater size expansion occurred at the vertical direction. This indicates that the volume of sprayed ink was too high for 0.10 mm layer thickness (low level) samples, and the extra ink penetrated the powder bed driven by gravity and diffusion, which finally resulted in the size expansion dramatically at vertical direction and slightlyat horizontal direct. In representative SEM images it can be observed that the 10% w/w of PVP sample (Fig. 5A), where crystals of undissolved PCM and coarse particles of lactose were visible, comprised more pores than the 30% w/w of PVP sample (Fig. 5B). The 30% w/w of PVP sample had a microstructure of agglomerated clots with some undissolved drug crystals. On the clots, there were near-spheric holes resulted from the hollow structure of primary PVP particles. SEM images show that the 30% w/w of PVP sample was more condensed than the 10% and 20% w/w of PVP samples (Fig. 5C). This confirms that the size shrinkage of printed products is due to a decrease in porosity of solid materials influenced by the binder content. The two phenomena (size expansion and shrinkage) impact the sample dimension accuracy and microstructure in the opposite directions, and their dominance is determined by the nature and the composition of primary powder and ink. Size expansion is not desired, since it can cause the failure of printing as discussed in *3.2.1 Ibuprofen products*. The size shrinkage mainly happens during drying (50 °C for 12 hours in this study) when printing is done. As indicated by the TGA result (Table 4, Residual water content %), all the final samples had slightly higher residual water content than raw materials of PCM (0.0 ± 0.0) and lactose (0.8 ± 0.1%) but lower content than PVP (7.4 ± 0.9%) as starting materials.

Since these two factors (binder content and layer thickness) also interacted in the model of diameter accuracy, the phenomena of size shrinkage and expansion might be more complicated to explain. For example, the response of weight, which was affected by all the three factors, was also strongly correlated to the diameter accuracy (Table S4).

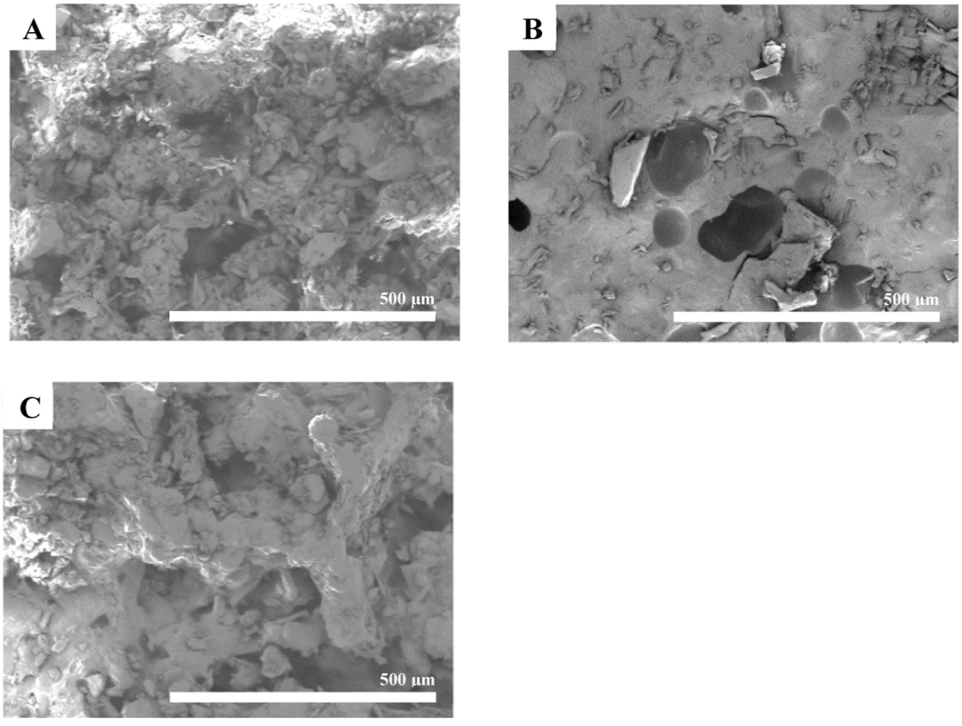

Fig. 5. Representative SEM images of printed paracetamol (PCM) products (A) PCM_3:1:6_0.10 mm*30, (B) PCM_3:3:4_0.10 mm*30, and (C) PCM_3:2:5_0.15 mm*35. Sample code follows Drug_DrugLoad:Polyvinylpyrrolidone:Lactose_LayerThickness*LayerNumber.

This indicates a connection between printed product density and the size shrinkage, both being related to the binder content. Hence, it can be concluded that 100% size accuracy of printing can be difficult to achieve as the complex nature of particle-ink interactions that are affected by multiple factors, and their influence on the size of printed product can cause the failure of printing or compromise the uniformity.

Regarding the drug loading that was supposed to be 100% for a homogeneous and perfectly filling primary powder, all the samples were within 100 ± 5% except for the sample of PCM_3:3:4_0.20 mm*40. Coefficients of the three factors (binder content, layer thickness, and layer number) in the statistical model for the drug loading (Table S3) indicate that a high PVP content in matrix, as well as a thick layer and/or a large number of layers, can cause a decrease on the percentage of PCM loaded in the printed products. The response of drug loading was strongly correlated to the weight of printed product (Table S4) since the two responses were both affected by all the three factors. The deviation on drug loading can be resulted from the segregation of particles with a different size. Infanger *et al.* (Infanger et al., 2019) reported that the sample with the largest particle size difference in their study showed the largest decrease on drug loading by the segregation effect. When the roller spreads fresh layer on printed area, undissolved particles in previously wetted powder bed can stick to the fresh powder and result in inhomogeneity in primary powder (Mostafaei et al., 2021). As the layer thickness and number of layers were studied at different levels, the degree of segregation variated. This remains a topic for further studies.

3.3.3. *Critical overview to the model*

Overall, the BJ 3D printing process involves several steps: ink spreading, powder wetting, imbibition, and absorption, followed by dissolution on binder and other materials, which all contribute to the formation of solid bridges after evaporation of the ink (Goole and Amighi, 2016, Mostafaei et al., 2021, Lu et al., 2009). These steps are driven by physical forces including capillary action, diffusion, and gravity that are determined by various material attributes, including primary powder composition, bulk and particulate properties, ink properties, and weight ratio of powder to ink. Besides the evident impact of binder content on product integrity, three other phenomena were identified affecting the product CQAs, namely, dissolution of powder materials leading to formation of liquid bridges, too high volume of ink penetrating the powder layer, and the size shrinkage due to the formation of solid bridges (Fig. 6). Material selection, a robust control of weight ratio of powder to ink, and setting proper product dimensions are important for assuring the quality of the printed products.

Moreover, an important practical step in BJ 3D process is the removal of printed products from powder residue. In this study, this step was conducted manually, and it was observed that with some samples, the boundary between printed region and powder residue was uncertain. It was further observed that some powder clots were stuck on the surface of the printed products, which required a manual removal of these particles. These clots can be formed by too high volume of ink that is binding extra particles (Mostafaei et al., 2021). This manual work might compromise the uniformity, which is the reason why the standard deviations of weight of all the printed products were close to or higher than 5%. Such problem can reduce the robustness of BJ method in fabricating uniform products. This is underpinning the importance of selecting the right weight ratio of powder to ink that can be achieved by ink volume or layer thickness. This is not a challenge when BJ 3D printing metal and ceramic materials, where the ink volume is only determined by the binder saturation level calculated by material porosity (Mostafaei et al., 2021, Lu and Reynolds, 2008). With pharmaceutical materials, the solubility and dissolution rate of materials should be always considered.

4. Conclusions

A structured approach according to QbD principles was implemented for BJ 3D printing of an analogue of pharmaceutical tablet for oral delivery. Based on the QTPP of the solid product and its qualitative risk assessment, CQAs including disintegration time, tensile strength, friability, diameter accuracy, height accuracy, residual water content, weight, and drug loading were identified as responses. Factors related to API and binder (i.e., the primary powder composition), the type of ink, and product dimensions were explored using factorial design. It was found that the PVP content in the primary powder was critical to the integrity related characteristics. During the solidification of particles in the primary powder, size expansion and shrinkage occurred simultaneously, which contributed to the final microstructure of the printed products. To control this, weight ratio of powder to ink and product dimensions were two CPPs. Primary powder with a broad particle size distribution is favorable as it can increase the powder bed density and

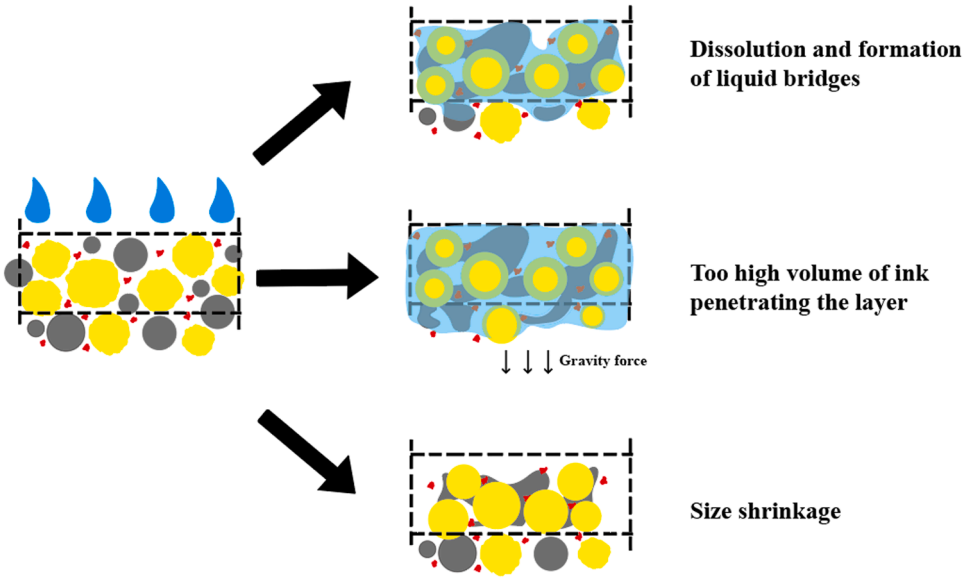

Fig. 6. Schematic illustration of the physical phenomena occurring during binder jetting 3D printing process. The blue droplet is illustrating ink, the grey solid circle is polyvinylpyrrolidone particle, the yellow solid circle is lactose particle, the red dot is paracetamol, and the black square in dash line is referring to the designed printed area. (For interpretation of the references to colour in this figure legend, the reader is referred to the web version of this article.).

improve power printability, but it might also cause the powder segregation leading to inaccurate drug loading in printed products. Finally, it can be concluded that acceptable PCM products can be fabricated by the BJ 3D printing technique. This study demonstrates the benefits of using a structured approach for designing a BJ 3D printed pharmaceutical product. It is of key importance to connect the experimental observations to the mechanisms related to solidification affecting the quality of printed products.

Funding

This research was fully supported by Mille International ApS, Hellerup, Denmark. This work did not receive any specific grant from funding agencies in the public or not-for-profit sectors.

Author contributions

Yingya Wang contributed on conceptualization, data curation, writing, and editing. Anette Müllertz and Jukka Rantanen contributed on conceptualization, supervision, and reviewing on this work.

Conflict of interest

All of the authors (Yingya Wang, Anette Müllertz, and Jukka Rantanen) are inventors in the patent application CN113080253A.

Data Availability

Data will be made available on request.

Acknowledgments

Authors would like to acknowledge the financial support from Mille International ApS, Hellerup, Denmark for the PhD project of Y.W., the assistance from Dorthe Ørbæk on the installation of the printing equipment, and the donation of material from DFE Pharma.

Supplementary materials

Supplementary material associated with this article can be found, in the online version, at doi:10.1016/j.ejps.2022.106280.

References

Trenfield, SJ, et al., 2018. 3D printing pharmaceuticals: drug development to frontline care. Trends Pharmacol. Sci. 39 (5), 440–451. https://doi.org/10.1016/j.tips.2018.02.006.

Lepowsky, E, Tasoglu, S., 2018. 3D printing for drug manufacturing: a perspective on the future of pharmaceuticals. Int. J. Bioprint. 4 (1) https://doi.org/10.18063/IJB.v4i1.119.

Goole, J, Amighi, K., 2016. 3D printing in pharmaceutics: a new tool for designing customized drug delivery systems. Int. J. Pharm. 499 (1-2), 376–394. https://doi.org/10.1016/j.ijpharm.2015.12.071.

Prasad, LK, Smyth, H., 2016. 3D Printing technologies for drug delivery: a review. Drug Dev. Ind. Pharm. 42 (7), 1019–1031. https://doi.org/10.3109/03639045.2015.1120743.

Sen, K, et al., 2021. Pharmaceutical applications of powder-based binder jet 3D printing process – a review. Adv. Drug. Deliv. Rev., 113943 https://doi.org/10.1016/j.addr.2021.113943.

Rahman, Z, et al., 2020. Printing of personalized medication using binder jetting 3D printer. In: Faintuch, J, Faintuch, S (Eds.), Precision Medicine for Investigators, Practitioners and Providers, 1 ed. Academic Press, London, pp. 473–481.

Yu, LX, et al., 2014. Understanding pharmaceutical quality by design. AAPS J. 16 (4), 771–783. https://doi.org/10.1208/s12248-014-9598-3.

Juran, JM., 1992. Juran on Quality by Design: The new Steps for Planning Quality into Goods and Services, 1 ed. The Free Press, New York.

European Pharmacopoeia Commission, 2019. 2.9.3 Dissolution test for solid dosage forms. European Pharmacopoeia, 10th. European Directorate for the Quality of Medicines & Healthcare (EDQM), Strasbourg, France.

European Pharmacopoeia Commission, 2019. 2.9.1 Disintegration of tablets and capsules. European Pharmacopoeia, 10th. European Directorate for the Quality of Medicines & Healthcare (EDQM), Strasbourg, France.

European Pharmacopoeia Commission, 2019. 2.9.7 Friability of uncoated tablets. European Pharmacopoeia, 10th. European Directorate for the Quality of Medicines & Healthcare (EDQM), Strasbourg, France.

Fromm, JE., 1984. Numerical calculation of the fluid dynamics of drop-on-demand jets. IBM J. Res. Dev. 28 (3), 322–333. https://doi.org/10.1147/rd.283.0322.

Mostafaei, A, et al., 2021. Binder jet 3D printing—Process parameters, materials, properties, —modeling, and challenges. Prog. Mater Sci. 119, 100707 https://doi.org/10.1016/j.pmatsci.2020.100707.

Chang, S-Y, et al., 2020. Binder-jet 3D printing of indomethacin-laden pharmaceutical dosage forms. J. Pharm. Sci. 109 (10), 3054–3063. https://doi.org/10.1016/j.xphs.2020.06.027.

Lu, K, Reynolds, WT., 2008. 3DP process for fine mesh structure printing. Powder Technol. 187 (1), 11–18. https://doi.org/10.1016/j.powtec.2007.12.017.

Sen, K, et al., 2020. Formulation design for inkjet-based 3D printed tablets. Int. J. Pharm. 584, 119430 https://doi.org/10.1016/j.ijpharm.2020.119430.

Wilts, EM, et al., 2019. Comparison of Linear and 4-arm star poly(vinyl pyrrolidone) for aqueous binder jetting additive manufacturing of personalized dosage tablets. Acs Appl. Mater. Inter 11 (27), 23938–23947. https://doi.org/10.1021/acsami.9b08116.

Tian, P, et al., 2019. Applications of excipients in the field of 3D printed pharmaceuticals. Drug Dev. Ind. Pharm. 45 (6), 905–913. https://doi.org/10.1080/03639045.2019.1576723.

Tian, P, et al., 2018. Oral disintegrating patient-tailored tablets of warfarin sodium produced by 3D printing. Drug Dev. Ind. Pharm. 44 (12), 1918–1923. https://doi.org/10.1080/03639045.2018.1503291.

Yu, DG, et al., 2009. A novel fast disintegrating tablet fabricated by three-dimensional printing. Drug Dev. Ind. Pharm. 35 (12), 1530–1536. https://doi.org/10.3109/03639040903059359.

Wang, CC, et al., 2006. Development of near zero-order release dosage forms using three-dimensional printing (3-DP) technology. Drug Dev. Ind. Pharm. 32 (3), 367–376. https://doi.org/10.1080/03639040500519300.

Lee, KJ, et al., 2003. Evaluation of critical formulation factors in the development of a rapidly dispersing captopril oral dosage form. Drug Dev. Ind. Pharm. 29 (9), 967–979. https://doi.org/10.1081/DDC-120025454.

Rowe, C, et al., 2000. Multimechanism oral dosage forms fabricated by three dimensional printing™. J Control Rel. 66 (1), 11–17. https://doi.org/10.1016/s0168-3659(99)00224-2.

Kozakiewicz, M, et al., 2021. Binder jetting 3D printing of challenging medicines: from low dose tablets to hydrophobic molecules. Eur. J. Pharm. Biopharm. https://doi.org/10.1016/j.ejpb.2021.11.001.

Majd, F, Nickerson, TA., 1976. Effect of alcohols on lactose solubility. J. Dairy Sci. 59 (6), 1025–1032. https://doi.org/10.3168/jds.S0022-0302(76)84319-6.

Antic, A, et al., 2021. Screening pharmaceutical excipient powders for use in commercial 3D binder jetting printers. Adv. Powder Technol. 32 (7), 2469–2483. https://doi.org/10.1016/j.apt.2021.05.014.

Antic, A, et al., 2018. Exploring the 3D Printing Binder Jetting Process for Pharmaceutical Applications. Chemeca 2018. Institution of Chemical Engineers, Queenstown, New Zealand, p. 256. https://search.informit.org/doi/10.3316/informit.046122308680631.

Infanger, S, et al., 2019. Powder bed 3D-printing of highly loaded drug delivery devices with hydroxypropyl cellulose as solid binder. Int. J. Pharm. 555, 198–206. https://doi.org/10.1016/j.ijpharm.2018.11.048.

Miyanaji, H, et al., 2018. A new physics-based model for equilibrium saturation determination in binder jetting additive manufacturing process. Int J Mach Tool Manu 124, 1–11. https://doi.org/10.1016/j.ijmachtools.2017.09.001.

Bai, Y, et al., 2015. Effect of bimodal powder mixture on powder packing density and sintered density in binder jetting of metals. In: 2015 International Solid Freeform Fabrication Symposium: The University of Texas at Austin, pp. 758–771.

Zhou, Z, et al., 2014. Printability of calcium phosphate: calcium sulfate powders for the application of tissue engineered bone scaffolds using the 3D printing technique. Mater Sci. Eng. C 38, 1–10. https://doi.org/10.1016/j.msec.2014.01.027.

German, RM, Park, SJ., 2008. Handbook of Mathematical Relations in Particulate Materials Processing: Ceramics, Powder Metals, Cermets, Carbides, Hard Materials, and Minerals, 1 ed. John Wiley & Sons, Canada.

Tan, JH, et al., 2017. An overview of powder granulometry on feedstock and part performance in the selective laser melting process. Addit. Manuf. 18, 228–255. https://doi.org/10.1016/j.addma.2017.10.011.

Bai, Y, et al., 2017. Effect of particle size distribution on powder packing and sintering in binder jetting additive manufacturing of metals. J. Manuf. Sci. E-T Asme 139 (8). https://doi.org/10.1115/1.4036640.

Spath, S, et al., 2015. Impact of particle size of ceramic granule blends on mechanical strength and porosity of 3D printed scaffolds. Materials 8 (8), 4720–4732. https://doi.org/10.3390/ma8084720.

Lanzetta, M, Sachs, E., 2003. Improved surface finish in 3D printing using bimodal powder distribution. Rapid Prototyp J 9 (3), 157–166. https://doi.org/10.1108/13552540310477463.

Yu, DG, et al., 2009. Novel oral fast-disintegrating drug delivery devices with predefined inner structure fabricated by three-dimensional printing. J. Pharm. Pharmacol. 61 (3), 323–329. https://doi.org/10.1211/jpp.61.03.0006.

Vromans, H, et al., 1985. Studies on tableting properties of lactose. Part 2. Consolidation and compaction of different types of crystalline lactose. Pharm. Weekbl. Sci. 7 (5), 186–193. https://doi.org/10.1007/BF02307575.

ICH Q3C (R8) Residual solvents. Geneva: International Conference on Harmonization of Technical Requirements for the Registration of Pharmaceuticals for Human Use, 2009. EMA.
Beach-Herrera LE, et al. Method and system for forming a dosage form within a packaging. US20210393533A1. 15 Oct 2019.
Guy, A, et al., 2009. Handbook of Pharmaceutical Excipients, 6 ed. Pharmaceutical Press, American Pharmacists Association, London, Grayslake, Washington.
Lu, K, et al., 2009. Effect of particle size on three dimensional printed mesh structures. Powder Technol. 192 (2), 178–183. https://doi.org/10.1016/j.powtec.2008.12.011.